Thesis for Degree of Master

Supervisor: Prof. Seong Jung Kwon

STUDY ON THE SIGNAL ANALYSIS OF SINGLE Pd NP COLLISION ON CARBON FIBER, Cu, Au AND Pt ULTRAMICROELECTRODES

Submitted by

RUDAKEMWA Hubert

August, 2021

Department of Chemistry

Graduate School of Konkuk University

STUDY ON THE SIGNAL ANALYSIS OF SINGLE Pd NP COLLISION ON CARBON FIBER, Cu, Au AND Pt ULTRAMICROELECTRODES

A Master's Thesis

submitted to the Department of Chemistry

and the Graduate School of Konkuk University

in partial fulfillment of the

requirements for the degree of

Master of Science.

Submitted by

RUDAKEMWA Hubert

May, 2021

This certifies that the Thesis of

RUDAKEMWA Hubert is approved.

Approved by Examination Committee

Chairman _____

Member _____

Member _____

June, 2021

Graduate School of Konkuk University

TABLE OF CONTENTS

List of Tables

List of Figures

ABSTRACT

Study on the signal analysis of single Pd NP collision on Carbon fiber, Cu, Au and Pt ultramicroelectrodes

RUDAKEMWA Hubert

Department of Chemistry

Graduate School of Konkuk University

Recently, an electrochemical method for the detection a nanoparticle's (NP's) collision at the surface of an ultramicroelectrode (UME) was studied by the Bard group and others. (Bard et al. 2010, Compton et al. 2017) The observation of a unique NP collision through the electrocatalytic amplification (ECA) method is made possible by the right combination of a NP, an inert electrode, and an electrocatalytic reaction. Pd NP is one of the most widely used as an electrocatalyst owing to its versatile electrocatalytic activity. Various materials such as carbon fiber, (Daryanavard, Zare 2017) Au, (Park, Kim et al. 2018) and Ni (Oja, Wood et al. 2013) have experimentally served as the inert electrodes for the detection of single Pd NPs collisions.

The response type of the transient current by the single NP collision is affected various factors including the material of the UME. The transient current of a NP, which collided and stayed on the electrode surface, manifested a staircase response. On the contrary, a blip (spike) response resulted when the collided NP bumped out of the UME surface or underwent side reactions. Therefore, various factors such as the reaction rate, and applied potential, also can affect the types of current response of a single NP collision. The material of UME is a key element that determines the type of current response

in a single NP collision event. The observation of multiple types of current responses at different UMEs is probably caused by the different interaction mechanisms between the NP and the UMEs. The shape of transient current implied that the electrocatalytic ability of the NP did not change consistently or diminished. The continuous electrocatalytic reaction should be the reason why we observed a staircase response. Meanwhile, the blip response indicates the deactivation of the NPs for some various facts, such as the metal alloying between the NP and the UME or facts related to the adsorption impurity.

Therefore, the reciprocal interaction between the NP and UMEs or between the NP and the chemicals such as impurities or reaction products is a key element in the determination of the current response of a single NP collision. The electrode material does not only affect the current response; it can affect the collision frequency as well. The reason to this possibility is the fact that there is an interdependency between the collision frequency and the adsorption coefficient of the NP on the UME.

In this study, carbon fiber (C), copper (Cu), nickel (Ni), gold (Au), and platinum (Pt) were introduced as a new electrode material for the electrocatalytic activity study of a single Pd NP collision on various material. The current responses of the single Pd NP collision on the various electrode was investigated. The transient current by the Pd NP collision changed from staircase to blip response depending on the material and applied potential of UME. Also, an analysis and comparison of the frequencies and peak heights of the transient currents was carried out, indicating that they were significantly different from each kind of UME.

Keyword: Palladium nanoparticles, ultramicroelectrodes, Hydrazine, Single nanoparticle, Collisio

Chapter 1. Introduction

As it is known, electrochemistry is the branch of chemistry dealing with the interrelation of electrical and chemical effects (Faulkner, Bard 2002). And nowadays, there is a growing trend of relying on electrochemistry to study nanoparticles (NPs) and their different possible applications.

Given that there are many electrochemical methods used in electrochemical research, it could also be implied that many of these methods are as well used in nanoparticle-related research. While many electrochemical methods are aimed at investigating (analyzing) and others at producing (synthesizing) new compounds, not all those techniques are necessarily used in nanoparticle collision research. While most of the electrochemical techniques used in laboratories of electrochemistry include potentiometry, amperometry, coulometry, voltammetry techniques (cyclic voltammetry, polarimetry, NPV, DPV, …), AC impedance spectroscopy, and scanning electrochemical microscopy (SECM) (Faulkner, Bard 2002, Mandler 2010); the two most used techniques in nanoparticle collision research are cyclic voltammetry and amperometry.

Like it was previously mentioned, there are currently growing trends in investigating the collision of various nanoparticles (NPs) at different ultramicroelectrodes (UMEs). Many such experimental investigations have been carried out. Some of the more prominent include the research with gold, platinum, and iridium oxide nanoparticles (Bard et al. 2010, Xiao, Fan et al. 2008, Xiao, Bard 2007, Kwon et al. 2010, Allerston, Rees 2018). The previously carried out research and more others have so far shown that it is possible to detect the collision of single NP at an UME. They have also shown that the type of current response observed does not only depend on the type of nanoparticles investigated, but also on the nature of the UME employed as

well as the nature of the reaction used during the electro detection (Bard et al. 2015).

Palladium (Pd) NPs have been found to possess some very unique properties that could present some very beneficial applications in the medical, industrial, environmental, and energy sectors (Chen, Ostrom 2015, Adams, Chen 2011, Yaqoob et al. 2020, Jiang et al. 2014, Stephen et al. 2019). Because of these reasons and other potential applications, many electrochemical investigations have been carried out. Some of these investigations focused on the preparations Pd NPs and their collisions on various UMES and in various electrochemical systems (Cookson 2012, Jiang et al. 2014, Hassan et al. 2018, Park et al. 2018). Although many such data have already been compiled, very More data on Pd NPs collision is also needed because Pd NPs could present some other very useful applications in the future.

Chapter 2. Theory

2.1. Cyclic Voltammetry

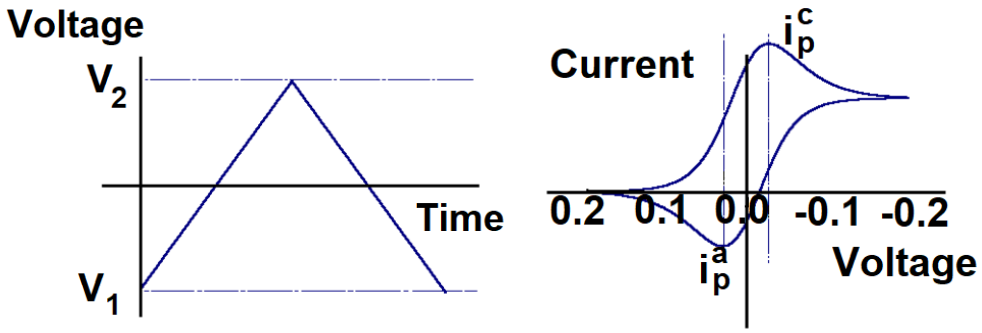

(a) (b)

Figure 1. Cyclic Voltammetry diagrams (a) potential variation as a function of time (b) representation of the current change as a function of voltage on the cyclic voltammogram

Among Electrochemical Techniques, Cyclic Voltammetry is very much relied upon to detect the electrocatalytic activities of many chemical species. The main advantage of this method in electrochemical analysis is its ability to provide the characteristics of an electrochemical system. In a CV experiment, a potential ramp is applied by the potentiostat to the working electrode to continuously vary the potential and, then returns the potential to its initial value by reversing the scan (see the triangular waveform in Figure (a) .

The relationship between the concentration of oxidizing species and reducing species is expressed with Nernst equation.

$$E = E_O + \frac{RT}{nF} \ln \frac{C_O}{C_R}$$

E_O = Formal potential of electrode

C_O = concentration of oxidising species

C_R = concentration of reducing species

F = the Faraday constant

2.2. Signal Amplification of the Single NP Collision

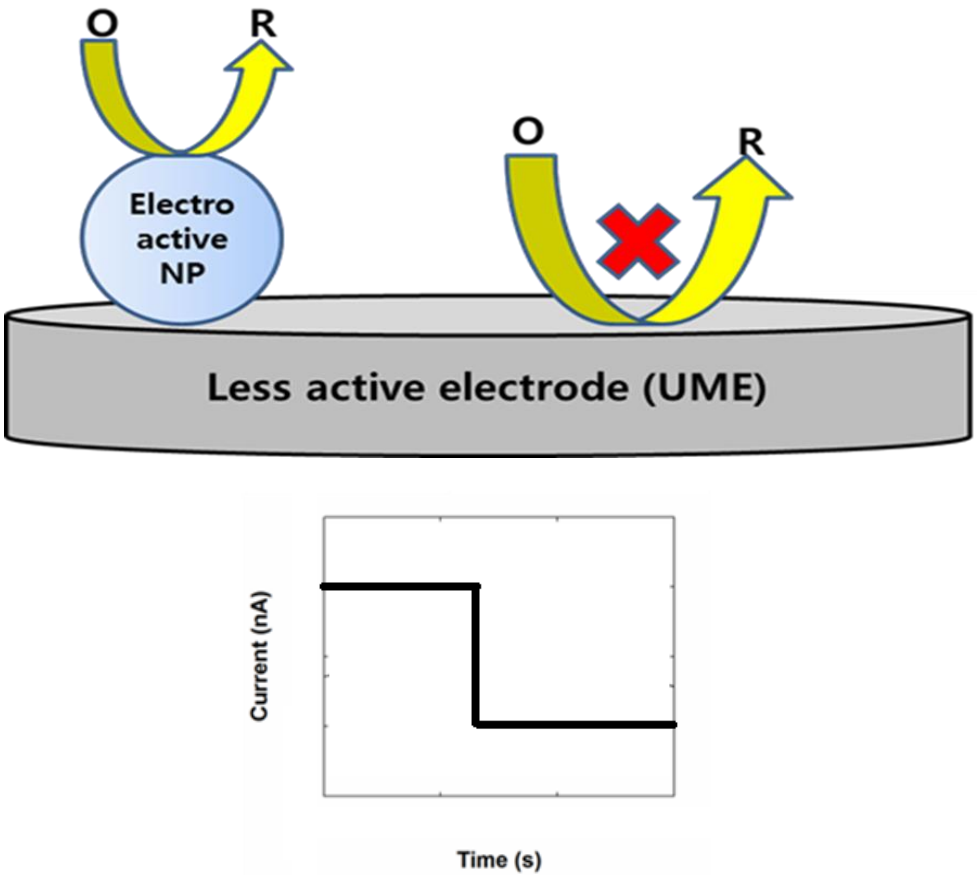

Figure 2. General representation of a sticky NP collision and the ideal current response

This is one the methods employed in the detection of nanoparticles. It relies mainly on the fact that once the nanoparticle touches the surface of the UME, some interesting phenomena may take place.

First, the surface area and topography of the electrode momentarily changes because the electroactive NP acts an additional surface for the electrochemical reaction. However, if the NP conducts the current as closely to the UME material, it will be very difficult to distinguish the new current from the background level or noise.

Otherwise, if the nanoparticle material is different and can catalyze a redox reaction, this will lead to a change in the amount of electrical current flow. If the current flow is higher enough, this will provide enough amplification of the signal and thus an easy detection of the of the signal nanoparticle collision.

When the NP is adsorbed on the electrode's surface, an additional steady-state current diffusion-controlled current can be produced by the NP. It is calculated by the following equation (Bard et al. 2015):

$$I_{SS} = 4\pi(\ln 2)nFDCr$$

$\boldsymbol{n}$ = number of electron
$\boldsymbol{F}$ = Faraday coefficient
$\boldsymbol{D}$ = the diffusion coefficient of hydrazine
$\boldsymbol{C}$ = the concentration of hydrazine
$\boldsymbol{r}$ = the radius of NP

The previous equation presents some dissimilarities with that for a spherical UME by the l*n*2 term, which stands for the fact that the supporting planar surface is blocking the diffusion path to the NP. When this happens, the current

from every new NP contact combines itself to the previous one and a *staircase* response results as shown in Figure 2.

When the NP does not remain attached to the electrode, the value of the total charge transferred is dependent by the speed of the electrocatalytic reaction, the speed of charge transfer from the electrode, the NP size, and its residence time on the electrode. When the non-attachment case happens, each new NP contact can cause a transient or *blip* current, on top or bottom of a constant background current.

When there is an irreversible sticking of the nanoparticles on the UME surface, a concentration slope is created. The calculation of the collision frequency can be carried out from the steady-state diffusion-controlled flux of particles:

$$J_p = \frac{4D_pC_p}{\pi a}$$

where:

J_p= the particle diffusion coefficient

C_p= the concentration of the particles in solution

a = the radius of the UME disk electrode

After some transformations of the above equation, we end up obtaining the following expression:

$$f_p = J_pA = 4D_pC_pa$$

The above frequency is an approximate value of the real frequency. The reason is that the shape and frequency of the current are influenced not only by the kind of NPs but also by the material of the measuring electrode's surface.

2.3. Diffusion Layer of Ultramicroelectrode

The sizes of commonly used electrodes and Ultramicroelectrodes (UMEs) are different. Commonly used electrodes have a relatively larger diffusion layer than UMEs. We consider an electrode as an UME if its diameter is less than ~25 μm.

The reaction at any electrode will be affected by mass transfer and the charge transfer. As the diffusion layer at any electrode changes, the mass transfer rate will also undergo some changes. Figure 3 shows how the diffusion layers look like in a typical electrode and an UME. As it can be noticed, at relatively larger electrodes, the chemical species undergo a linear diffusion whereas at the UME, the same chemical species will undergo a hemispherical diffusion.

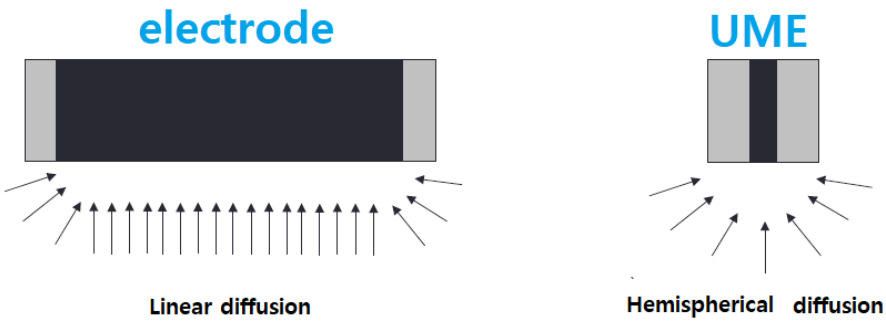

Figure 3. Diffusion layers of a large electrode and an UME

As a consequence of the previous phenomenon, cyclic voltammograms of UMEs will display shapes that are usually different from those of the normal electrodes. These different shapes are the result of different mass transfers in both electrodes. The larger the electrode surface is, the thickness of the

diffusion layer will be small relatively to the electrode diameter. And the mass transfer will occur more and more at right angles to the electrode surface. This phenomenon is depicted as semi-infinite linear diffusion and as it causes an exhaustion of the comparatively thin diffusion layer of redox active species, it also results in a transient current response (Walsh et al. 2010). Figure 4 (A) shows a typical CV response related to this case.

Concerning the cyclic voltammetry at a UME the case is more complex. With short timescales (high *u*), the diffusion layer keeps a small thickness compared to the diameter of the UME surface and a transient response (a CV like that shown in Figure 4 (A) can be displayed. In contrast to the previous case, at longer experimental timescales (low *u*), the thickness of the diffusion layer is larger than the diameter of the UME; and hemispherical diffusion to the UME is more pronounced. Here, the depletion of the diffusion layer of the redox-active species does not take place, and this causes a steady-state current response (Walsh et al. 2010). Figure 4 (B) shows a typical sigmoidal CV obtained at a UME.

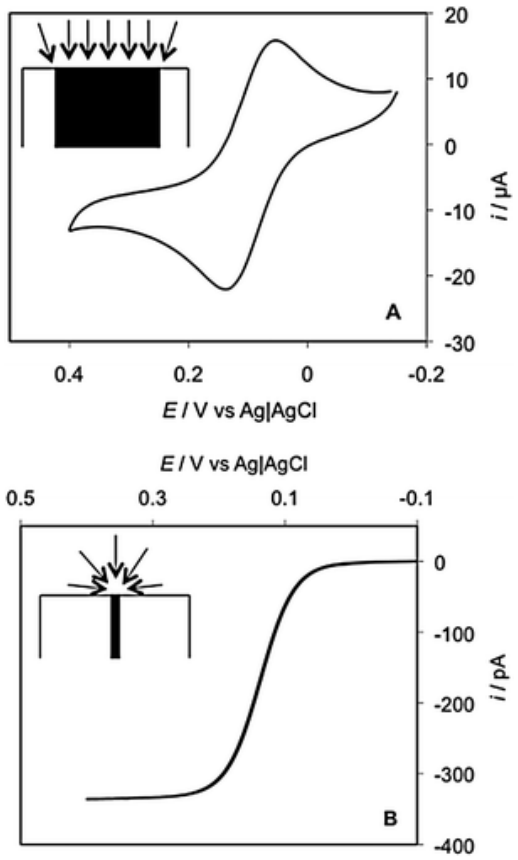

Figure 4. Typical cyclic voltammograms obtained (a) a 2 mm diameter Pt disk and (b) a 1.3 µm diameter Pt disk UME in 1 mM ferrocenemethanol dissolved in 0.1 M KCl. The scan rates, (a) 100 mV/s and (b) 5mV/s .

2.4. Types of Single Nanoparticles Collision Response

In regard to the signal responses that are obtained during the electrochemical experiments of NP collisions, it is important to mention that there are many types of signals that can be obtained. Each of these collision response types is generally depending on how the nanoparticle is adsorbed on the electrode surface, which in turn will also be affected by the types of UME material used and the type of reaction that take place (Bard et al. 2015, Cheng, Compton 2014).

Electrocatalytic Amplification

In the solution, NPs sometimes collide with an inert (less electrochemically active) electrode and make electrical contact (i.e., the NP stays within the tunneling distance), the behaviour of the NP is the same as that of a nanoelectrode. The detection of a single NP electrically in contact with a UME, relies on an IS electron transfer reaction, and it is also assumed that the reactant has strong interaction with the electrode material.

As a consequence, the value of the electrocatalytic current response changes with the electrode material.

For Amperometric collision detection that use electrocatalytic amplification (EA), one finds a suitable electrode potential where the particle materials provide its maximum current while a minimal current response is displayed by the inert electrode. As exposed in Figure 2.2 by the comparison of the electrochemical attitude of the targeted electrocatalytic reaction on two dissimilar electrode materials, the right potential to apply is easily found. Said otherwise, the catalytic difference between the two materials is used in the detection of catalytic NPs at a less catalytic electrode. Various IS reactions can be used to detect NPs.

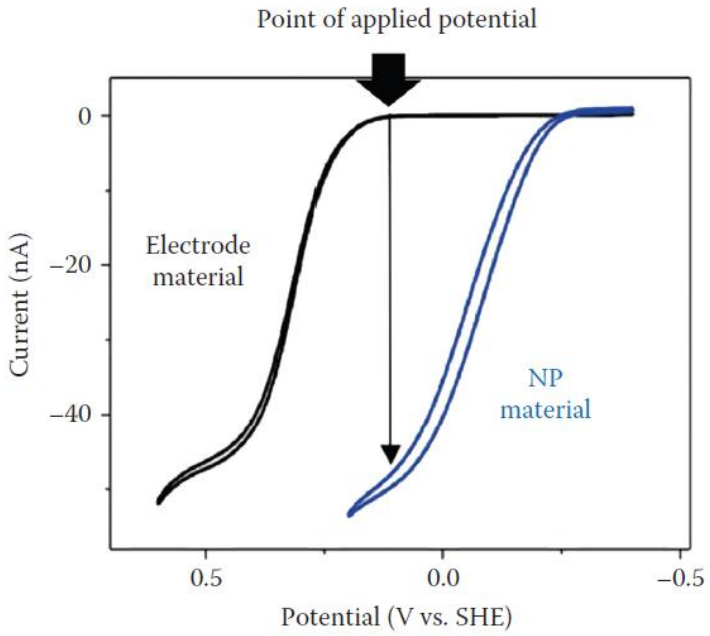

Figure 5. Schematic display of single NP detection principle using electrocatalytic differences of two materials.

Generally, it has been observed that each system can display a unique response that depends on the properties of the metal, reactant, reaction intermediate, and reaction environment. The types of current responses employed to detect NPs are detailed in the next sections.

Types of Current Responses

The kind of current response observed from the collision of a single NP depends on the strength of the adsorption of the NP on the electrode surface. The behaviour of an adsorbed NP is similar to that of a nanosphere electrode on an inert plane and it leads to the production of a step-like current increase. Estimation of the step height can be found from Equation X.1 when the rate of charge transfer from the NP to the solution species is fast (i.e., diffusion-limited conditions) :

$$I_{SS} = 4\pi(\ln 2)nFD_{rct}C_{rct}r_{NP}$$

n = number of electron

F = Faraday coefficient

D_{rct} = the diffusion coefficient of the reactant

C_{rct} = the concentration of reactant

r_{NP} = the radius of NP

A non-adsorbed NP or one that has been decomposed or whose surface has been deactivated can produce spike or blip responses. The shape as well as the residence time are affected depending on how the NP is adsorbed on the UME surface. The modification of the step current response can be caused by the entrapment of a bubble, the adsorption of impurities, the detachment of a NP, or the decomposition of a NP. Hence, the current response for single NP collisions differs for every system.

Staircase current response: Observation of a staircase current happens when there is a collision of the particles with the electrode surface; followed by a sticking (or adsorption) of these particles on the UME surface. A steady-state current response is obtained with the following electrocatalytic systems: proton reduction, hydrazine oxidation, and hydrogen peroxide reduction.

In a lot of situations, a current decay after collision events distorts the staircase current. This decay is due to a deactivation process, such as the adsorption of impurities, and the decay rate depends on the experimental conditions. Figure 6 illustrates some examples of Staircase current response from various systems.

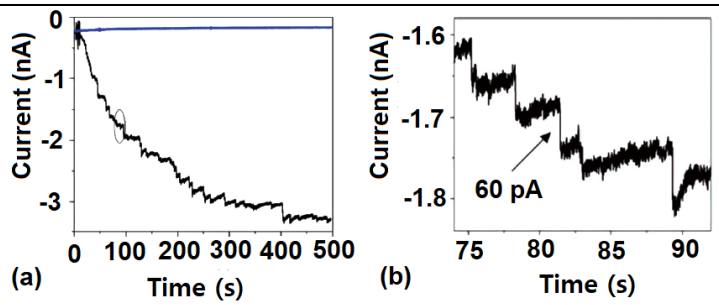

Pt NPs at the Au UME using the hydrazine oxidation reaction.

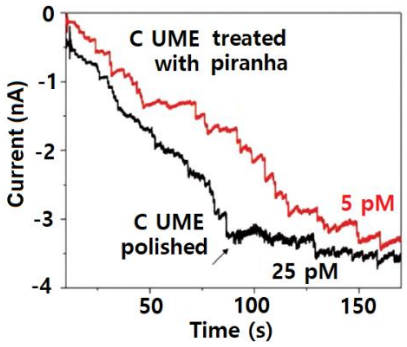

Pt NPs at the C UME using the hydrazine oxidation reaction.

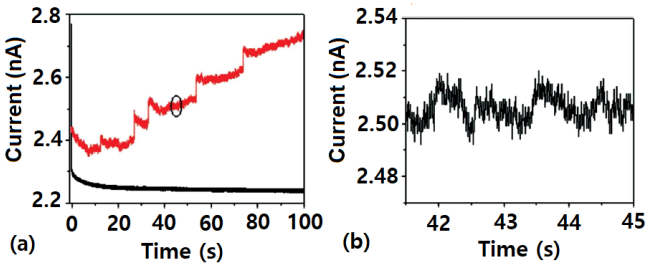

Pt NPs at the Au UME using the hydrogen peroxide decomposition reaction.

Figure 6. Examples of Staircase current response from various electrochemical systems.

Description of figure 6

Pt NPs at the Au UME using the hydrazine oxidation reaction. (a) Record of the current–time curve before and after injection of Pt NP solution in 50 mM phosphate buffer and 15 mM hydrazine, pH ~7.5. (b) Zoom in of panel (a).

Pt NPs at the C UME using the hydrazine oxidation reaction. Record of the current transients before and after injection of Pt NPs at a C UME polished (black) and treated afterwards with piranha solution (red). Electrode potential, 0.5 V; test electrolyte, 15 mM hydrazine and 50 mM phosphate buffer; Pt NP size, ~3.6 nm.

Pt NPs at the Au UME using the hydrogen peroxide decomposition reaction.(a) Current transients at a benzenedimethanethiol modified 25 μm diameter Au electrode at 0.1 V vs. SHE in 0.1 M phosphate buffer (pH 7.4) solution in which 50 mM hydrogen peroxide is dissolved, and with the absence (black) or presence of 25 pM Pt NP (red). To clarify the results, there was an increase of the background current in black curve by 1.5 nA. Part (b) is a zoom in of part (a).

Blip (or spike) current response: The observation of A *blip*-type response can sometimes happen when a particle makes electrical contact with the electrode surface only for a very short period. That is most often when the NP contacts the surface but is unable to stick well. For an elastic (i.e., nonsticking) collision event, the amperometric response should have a spiky shape and the width of that response should determine the particle residence time.

Whenever the NP does not irreversibly stick to the UME surface, the estimation of the collision frequency from the diffusion-controlled flux of NPs cannot be carried out because there is no generation of a concentration gradient.

In regard to the case of a blip response, the number of attached NPs on the UME cannot be estimated from the final current. This is contrasting with the current step response where an estimation of the number of attached particles can be made using the final current, assuming the particles have not undergone any deactivation process. However, systems exhibiting a blip-type response keeps on having a stable background current, which eases the distinction between the collision events and hinders the signal interference of consecutive NP collision. Therefore, NP detection based on blip-type responses can be advantageous in analytical applications such as those related to the investigation of the size distributions of NPs. Figure 7 illustrates some examples of Blip current response from various systems.

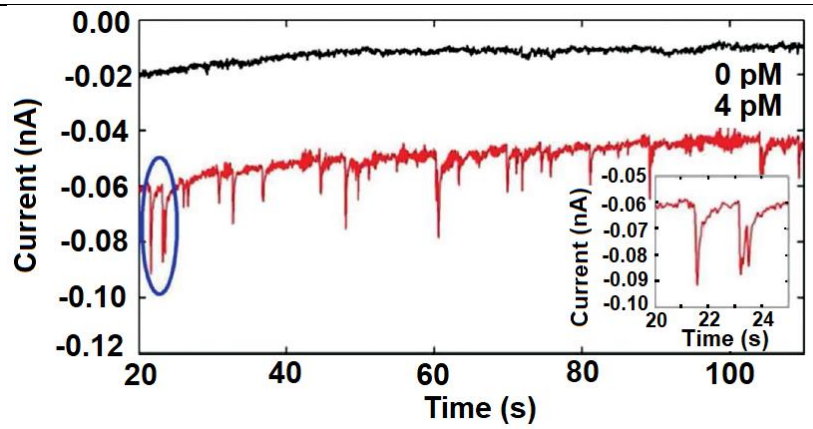

IrOx NP at the Pt UME using water oxidation reaction.

CA curves for single IrO_x NP (radius ~14 nm) collisions at the NaBH4-treated Pt UME of radius 5 μm, in 0.1 M NaOH (pH 13) solution with (red) and without (black) 4 pM IrO_x NPs. Data acquisition time: 50 ms. Applied potential: 0.8 V (vs. Ag/AgCl). The very little variation in the background current can be due to a small number of IrO_x NPs sticking to the electrode.

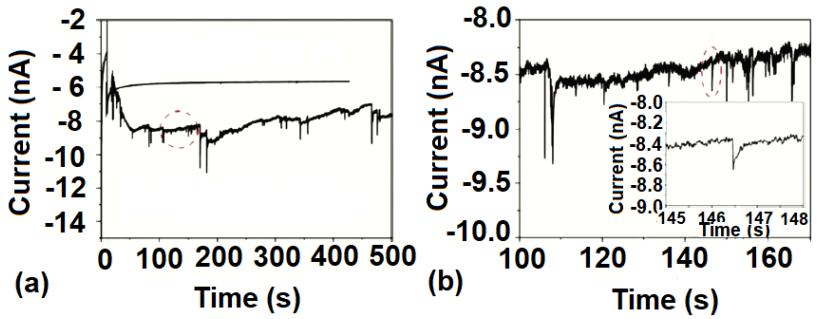

Au NPs at the Pt UME using the $NaBH_4$ oxidation reaction.

(a) CA curve with (bottom curve) and without (upper curve) injected Au NPs at the preoxidized Pt UME. (b) Zoom in of marked region in panel (a). UME diameter, 10 μm; potential, 0 V; NP concentration, 24 pM.

Figure 7. Examples of Blip current responses from various systems.

UME blocking response: A blocking response can be observed when the metallic nanoparticles are inactive or less electroactive while the UME has some more pronounced electrocatalytic character. In this case, each NPs act like a potential barrier for the electrochemical reaction. This means that the amperometric response of this collision should be opposed to the signal of the electrocatalytic amplification when the NPs gets in contact with the UME surface. The surface blocking will decrease the already existing electrocatalytic current. Observing the blocking response type from another point of view, it can seem as if the background current decreases whenever a nanoparticle hits the surface of the UME. Figure 8 illustrate an example of blocking current response in an NP-collisions electrochemical detecting system (Sundar et al. 2019, Mun et al. 2017).

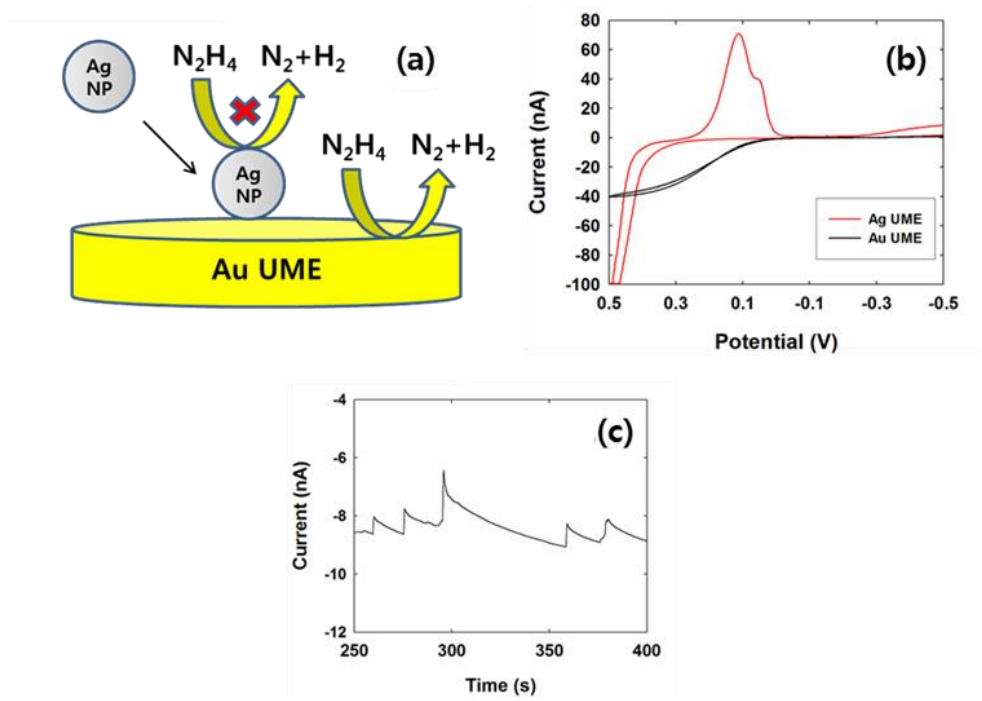

Ag NPs at an AU UME using the hydrazine oxidation reaction.

(a) schematic illustration of a single Ag NP collision event (b) The electrochemical oxidation of hydrazine at Au UME (black) and Ag UME (red) in pH 7 solution (50 mM PB Buffer). Scan rate is 50 mV/s. (c) Chronoamperometric curves for single Ag NP collisions at the Au UME with Ag NPs. Applied potential is 0.3 V (vs. Ag/AgCl). Data acquisition time is 50 ms.

Figure 8. Example of a UME blocking response.

Chapter 3. Experimental Procedure

3.1. Reagents

Our experiments were performed with the following reagents:

Palladium (II) Chloride ($PdCl_2$, 99%); Citric Acid ($C_3H_5O(COOH)_3$, ≥99.5%); Sodium Borohydride ($NaBH_4$, ≥ 96%); Potassium Phosphate monobasic (KH_2PO_4, ≥ 99.0%); Potassium Phosphate dibasic (K_2HPO_4, ≥ 98%); Hydrochloric Acid (HCl, 35.0-37.0%). Apart from Hydrochloric acid which is from SAMCHUN, all other previous reagents are from SIGMA-ALDRICH. In all our experiments, we also used Ultrapure water (≥18MΩ, Millipore).

3.2. Preparation of Pd Nanoparticles

The experiments we performed specifically passed through the following steps:

- Nanoparticle Synthesis (Pd)
- UMEs Production (Cu, Ni, Au, Pt, Pd)
- Collisions experiments (Hydrazine)

3.2.1. General Standard Procedure

- Prepare 20 mL of 1 mM HCl.
- Dissolve 1.773 mg of $PdCl_2$ in the 20 mL of 1 mM HCl under ultrasonic treatment for 30 min.

- After that, dissolve 3.842 mg of citric acid (1 mM) in the mixed solution with magnetic stirring for 5 min at 80^0C.
- Finally, add slowly 2 mL of 0.1 M $NaBH_4$ aqueous solution to the mixture under magnetic stirring. The color of the solution should become dark brown.

Figure 9. Prepared palladium nanoparticles

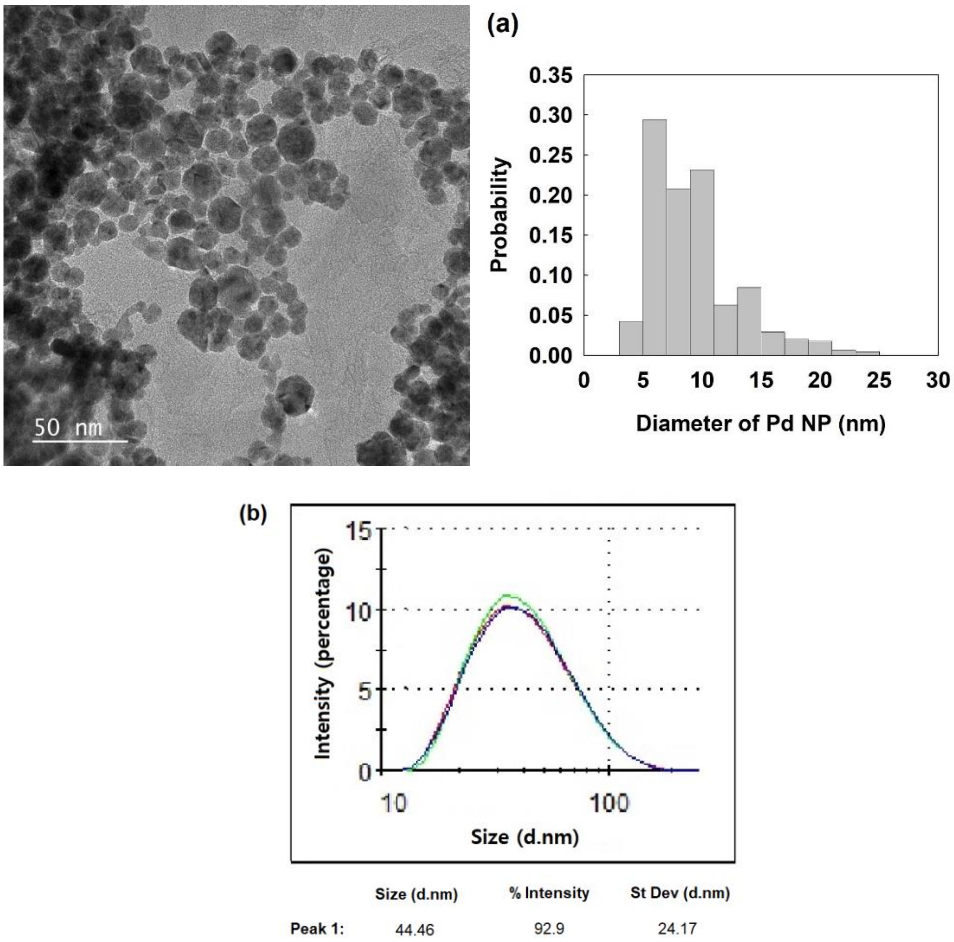

Figure 10. TEM and DLS data of the Palladium nanoparticles
(a) TEM picture and Particles count of Pd NPs (b) Pd NPs DLS size distribution

3.2.2. Various Molar Ratios

The synthesis of palladium nanoparticles referred to in section 3.2.1 uses the molar ratios of 1-20-2 (see Table 1). To prepare solutions of Palladium nanoparticles with different molar ratios, the following procedures can be used:

- Prepare 20 mL of 1 mM HCl.
- Dissolve **X mg of $PdCl_2$** in the 20 mL of 1 mM HCl under ultrasonic treatment for 30 min. The values of X corresponding to each molar ratio are in Table 2.
- After that, dissolve **Y mg of citric acid** (1 mM) in the mixed solution with magnetic stirring for 5 min at 80^0C. The values of Y corresponding to each molar ratio are in Table 2.
- Finally, add 2 mL of **[mz] M $NaBH_4$ (Z mg of $NaBH_4$ in 2mL of Water)** aqueous solution was slowly to the mixture under magnetic stirring. The color of the solution should become dark brown. The values of Z corresponding to each molar ratio are in Table 2.

After using this procedure, we obtained various solutions of Palladium nanoparticles with different molar ratios (see figures 11 and 12). DLS data showed that the size distributions of different nanoparticles change with the molar ratios (see Table 3).

Reagent	$PdCl_2$	$NaBH_4$	Citric Acid
Molar masses	177.31 **g/mol**	37.83 **g/mol**	192.12 **g/mol**
Number of Moles	9.99943601607 e-6	2.002114723764 e-4	1.999791796793 e-5
Molar Ratios (accurate)	1	20.022	1.999
Molar Ratios (Approxima-tion)	1	20	2

Table 1. Original calculations for various molar ratios

Reagent	$PdCl_2$	$NaBH_4$	Citric Acid	Molar Ratio
Molar Ratio	1	20	2	
Mass to use (/2)	0.0008865 g	0.003787 g (99%)	0.001921 g	**1:20:2**
Molar Ratio	1	18	1.8	
Mass to use (/2)	0.0008865 g	0.0034083 g (99%)	0.0017289 g	**1:18:1.8**
Molar Ratio	1	16	1.6	
Mass to use (/2)	0.0008865 g	0.0030296 g (99%)	0.0015368 g	**1:16:1.6**
Molar Ratio	0.9	20	2	
Mass to use (/2)	0.0007978 g	0.003787 g (99%)	0.001921 g	**0.9:20:2**
Molar Ratio	0.8	20	2	
Mass to use (/2)	0.0007092 g	0.003787 g (99%)	0.001921 g	**0.8:20:2**

Table 2. Various values for the new molar ratio calculations

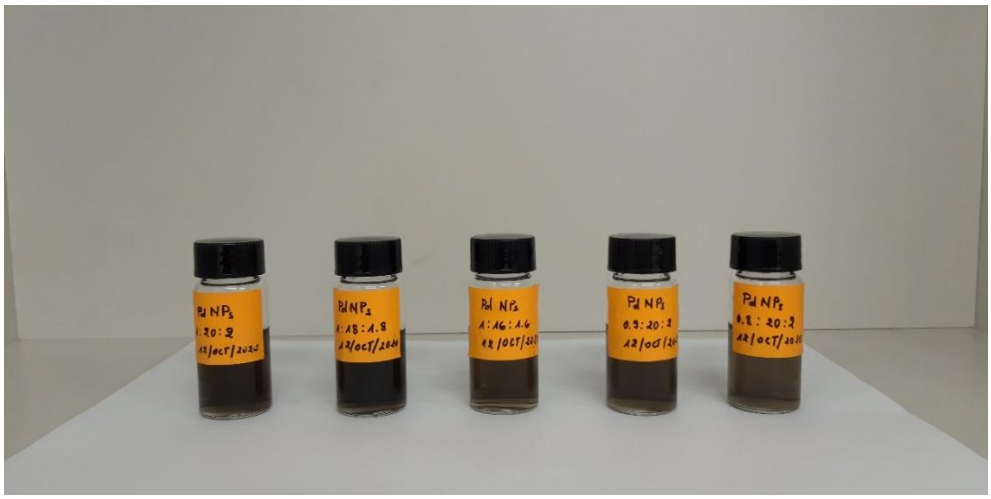

Figure 11. Prepared Nanoparticles Solutions (Front View)

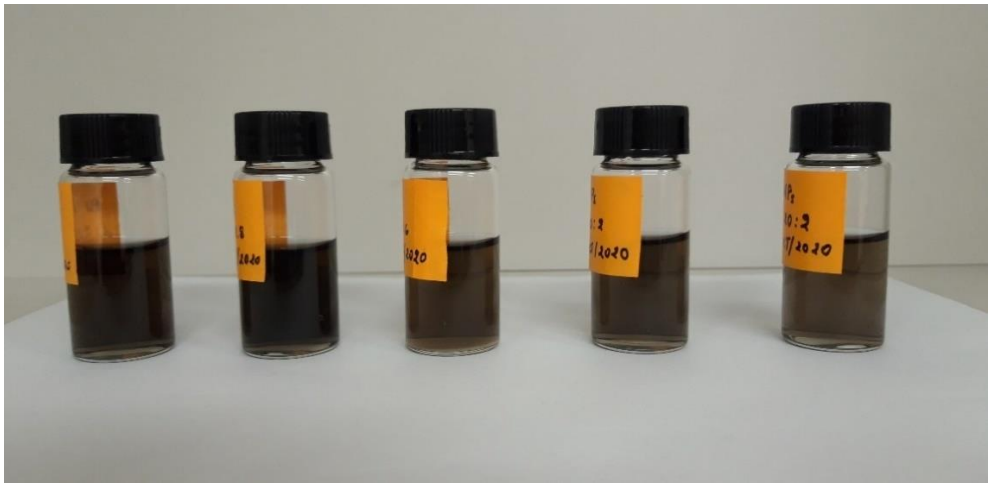

Figure 12. Prepared Nanoparticles Solutions (Side View)

Method of Preparation	PdNps Sample Name	Value 1	Value 2	Value 3	Average Value
3.2.1.	PdNps 1:20:2	59.86	60.51	58.96	59.8
3.2.2.	PdNps 1:18:1.8	82.41	80.38	81.02	81.3
	PdNps 1:16:1.6	41.02	40.51	41.41	41.0
	PdNps 0.9:20:2	62.32	61.45	61.45	61.7
	PdNps 0.8:20:2	118.3	115.8	97.48	110.5
3.2.3.	PdNps 1:20:2	43.86	43.90	44.90	44.22

Table 3. Nanoparticles size distributions obtained from DLS Analysis. Values indicated in the Table are Z-Average diameter length in nanometer.

3.2.3. Dilution Method

This method decreases the number of errors that be introduced by the pipetting of very little volumes of reagents. Therefore, it allows more accuracy to be reached experimentally. It can be adapted for the standard amount or the various molar ratio of palladium nanoparticles. Here down is the presentation of its adaptation in the preparation of the general standard amounts.

- Prepare 120 mL of 0.02 M HCl.
- Prepare an already mixed mother-solution 10 mM of H_2PdCl_4 aqueous solution by dissolving completely 88.6 mg of $PdCl_2$ in 50 mL of 20 M HCl under ultrasonic treatment for 30 min.
- Mix successively 1 mL of the mother-solution, with 19 mL of distilled water, and 3.842 mg of Citric Acid to obtain 20 mL of the intermediate solution.
- Mix the content of the intermediate solution under a hot bath at 95°C for 5 min.
- Finally, add 2 mL of 0.1 M $NaBH_4$ aqueous solution to the mixture under magnetic stirring. The color of the solution should become dark brown after each mixing.

The results presented in the present scientific research were carried out with the nanoparticles obtained while using the preparation method 3.2.3.

3.3. Preparation of Ultramicroelectrodes (UMEs)

The preparation of the ultramicroelectrodes is carried out according to the following steps. Steps 1&2: The Borosilicate glass is first heated with a torch. Step 3: Then the metal wire of interest (dia. ~ µm) is inserted in the borosilicate glass. Step 4: After that, the end of the glass tube containing the metal wire undergoes a heating with a resistance nichrome wire. Step 5: At the end of the previous heating, a part of the Metal wire Exposed while the other one is adhering to the glass tube. Step 6: The following step is to insert a silver paste inside the glass and insert another larger wire inside the silver paste. Step 7: The next step is to use Sandpaper to remove the excess glass tube and polish the exposed tip with alumina powder. Step 8: The surface area of the UME is checked with standard redox electrochemistry of ferrocene methanol. The carbon-fiber UME was not prepared according to the previously described method. It was pre-purchased from BASI (west Lafayette, IN, USA).

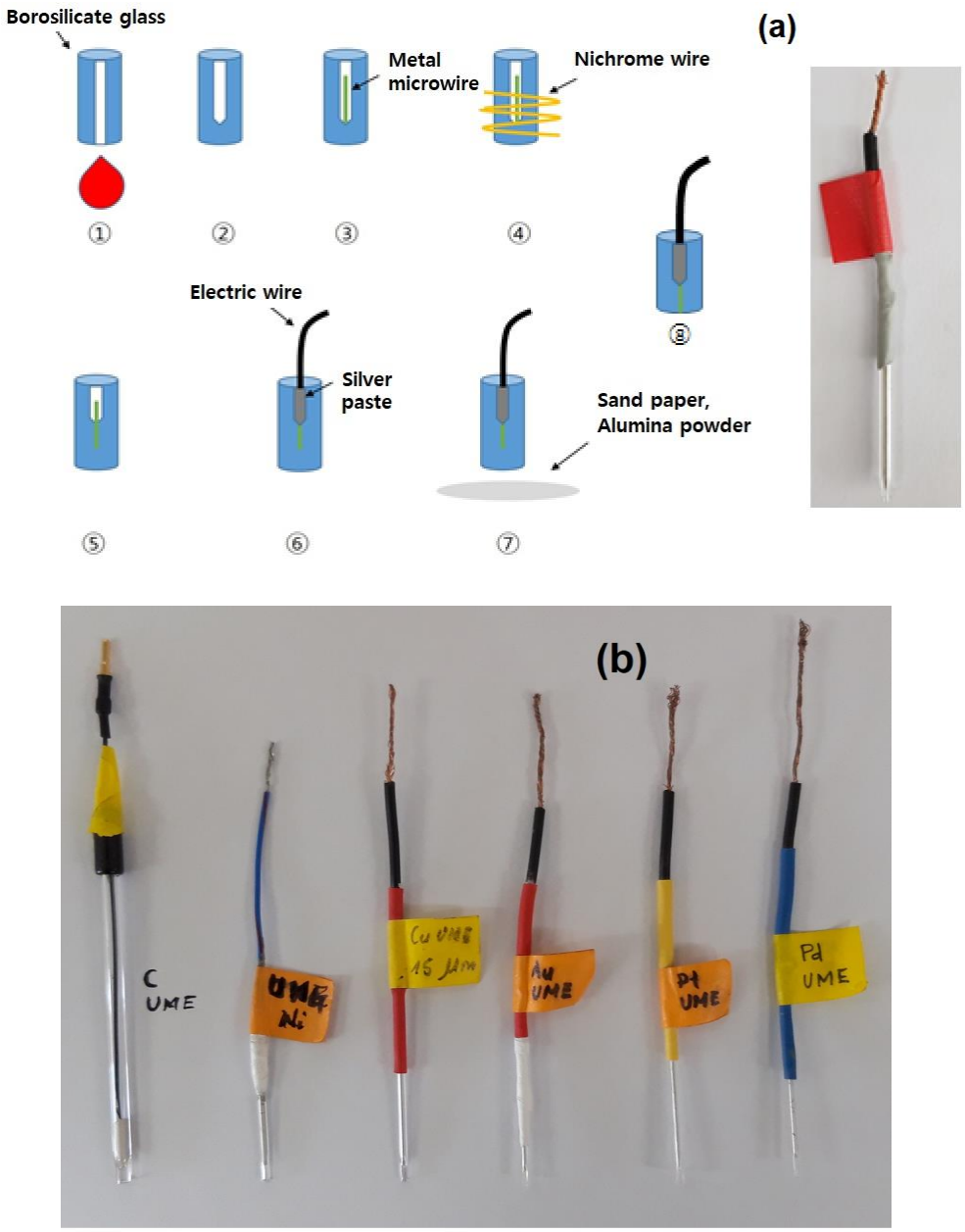

Figure 13. Ultramicroelectrodes (UMEs)

(a) The making process (b) C, Cu, Ni, Au, Pt and Pd UMEs

3.4. Apparatus

The apparatus used in our Collision detection response is a CHI 660A electrochemical Workstation (CH Instruments). A conventional three-electrode cell under room temperature was used for all the experiments. Depending on the experiment carried out the working electrode (WE) was either a Carbon fiber, Copper, Nickel, Gold or Platinum ultramicroelectrode (UME). A platinum electrode was always used as the counter electrode (CE) and a 1 M KCl Ag/AgCl electrode as the reference electrode (RE). In all the amperometry experiments were carried out in 0.05 M Phosphate buffer (PB) solutions. All the experimental environment was enclosed inside a Picoamp Booster & Faraday Cage.

Chapter 4. Results & Discussion

As previously mentioned, the detection of all the single nanoparticle (NP) collisions involved our research was conducted using the electrocatalytic (ECA) method. This method relies on the fast electrocatalytic reaction that happens during the collision of an NP with the targeted ultramicroelectrode (UME). Our targeted UMEs were carbon fiber (C), copper (Cu), nickel (Ni), gold (Au), and platinum (Pt) UMEs. As it is generally known, the electrocatalytic current difference for hydrazine oxidation between a Pd NP and the targeted UME should be maximized for the successful observation of a Pd NP collision on the targeted UME. To detect the right potential for this, the electrocatalytic activity of Pd UME for the hydrazine oxidation was first searched and its value was compared with those of Carbon fiber, Cu, Ni, Au, and Pt UMEs.

From figure 14, it can be observed that the general behavior of all the curves of hydrazine oxidation on the C, Cu, Ni, Au, and Pt UMEs differ significantly from that on a Pd UME. Au and Pt UMEs display almost the same electrocatalytic activities for the hydrazine oxidation in the regions between 0.5 V and 0.3 V (vs Ag/AgCl). It has however been observed that there are some very close similarities between the cyclic voltammograms (CVs) of Pt and Pd UMEs in the regions of the applied potential between 0.1 V and -0.5 V. The Carbon fiber, Cu, and Ni UMEs do not show consistent electroxidation of hydrazine in the potential range -0.5 V and 0.5 V (vs. Ag/AgCl). There is however some small oxidation current rising near -0.2 V at the Cu UME, as represented in the inset of Figure 14.

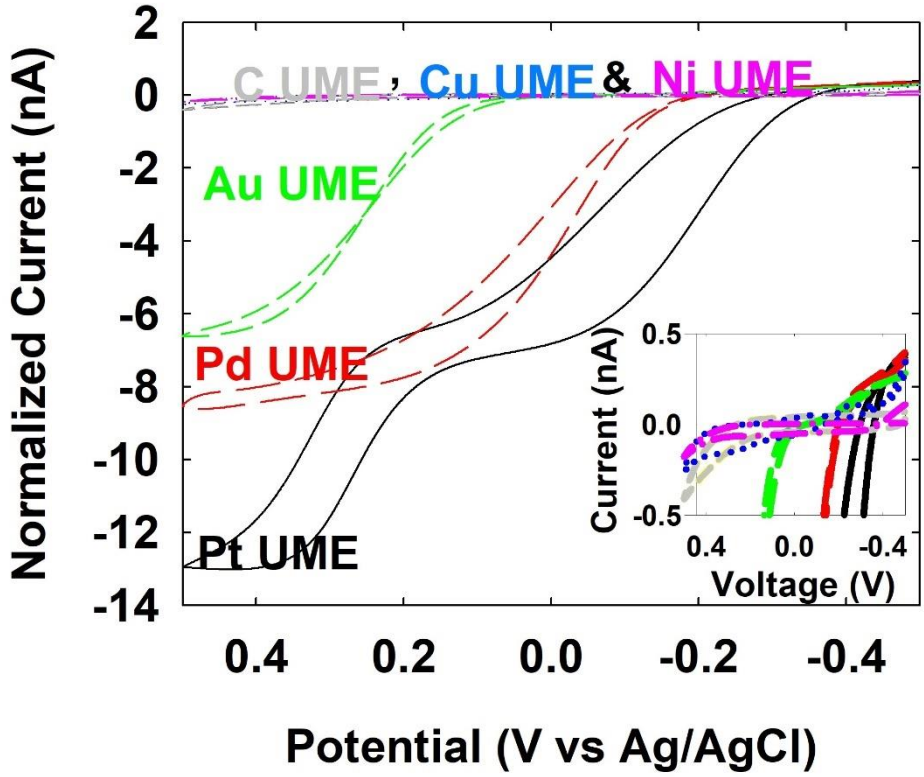

Figure 14. Cyclic voltammograms of hydrazine oxidation on carbon (gray, diameter 11 μm), Cu (blue dotted, diameter 15 μm), Ni (pink dash-dotted, diameter 25 μm), Au (green dashed, radius 25 μm), Pt (black solid, diameter 25 μm) UME, and Pd (red long-dashed, diameter 20 μm) UME.

In this regard, the small oxidation current observed on the Cu UME near -0.2 V seems to be due to the oxidation Cu electrode itself (Jung et al. 2016, Choi et al. 2014). As previously indicated, Carbon fiber, Cu, Ni presented very little activity for the hydrazine oxidation over the whole investigated range of -0.5 V and 0.5 V. Thus, it was predictable that these electrodes can present a large potential range for the single Pd NP collision due to the low

electrocatalytic activity for the hydrazine oxidation. To find the maximum current difference at the two materials, the potential of 0.1 V was applied to the Carbon fiber, Cu, Ni, Au, and Pt UMEs for the chronoamperometry (CA) measurement. At 0.1 V, we did observe some transient signals with C and Ni UMEs. These signals in C and Ni UMEs look at certain times blip-like and at other times staircase-like. At the same voltage as before, we did observe very little occurrence of hydrazine oxidation related to the collision of Pd NPs on the Cu UME. In many previous studies, single Au, Pt, and Ag NP collisions were observed using a C, Cu, and Ni UMEs and these studies revealed that different metal nanoparticles have the potential to undergo detectable collisions on these UMEs. (Sundar et al. 2019, Mun et al. 2017, Jung et al. 2016)

However, when it comes to the Au and Pt UMEs; it is important to note that they also show considerable electrocatalytic activity for the hydrazine oxidation, as shown in Figure 14. The Pt UME even displays almost similar electrocatalytic activity for the hydrazine oxidation as the Pd UME does if the potential is between 0.1 V and -0.5 V; and more electrocatalytic activity for the hydrazine oxidation more than the Pd UME does if the potential >0.1 V. Thus, the potential that can be applied to the Au UME for the CA measurement is limited to some potential values of voltages where the electrocatalytic hydrazine oxidation is sluggish at Au UME, usually at <0.1 V. Predictions suggest that if the potential is >0.1 V the hydrazine oxidation at an Au UME occurs actively, thus increasing the background current level. This can make it not easy to differentiate the small current signal by a single Pd NP collision with the background noise current created by the Au UME. It is also important to note that the background current at the Carbon fiber, Cu, and Ni UMEs is low over a wide range of potential. Thus, the CA measurement can be carried out if the applied potential on Carbon fiber, Cu, and Ni UMEs is greater than 0.1 V. As previously mentioned, during our introductory part, all our collision experiments were carried out exactly at 0.1V. We were greatly concerned with

what might happen if one operated the amperometric measurements exactly at 0.1 V instead of a relatively higher but closer values. Amperometric measurements at a higher voltage (0.3 V) were also carried for a matter of comparison.

In addition, given the very large electrocatalytic activity displayed by the CV of the Pd UME for the hydrazine oxidation, it can be predicted that single collisions of Pd NPs would always be detected especially when getting in contact with less electroactive UME materials such as Carbon fiber, Cu and Ni UMEs. The experimental results show that the above assertion could only be realized with only Carbon fiber and Ni UME materials. Previous studies have shown that under slightly different conditions, the collision signals can also be observed on Cu UME material. The fact that Cu UME materials did show very little collision current signals in our experiments may be attributed to a lack of suitable adsorption of the Pd NPs on the surface of the Cu electrode under the application of the 0.1 V potential.

Regarding the Pt UME, we had previously mentioned that it displays particularly the same electrocatalytic activity for the hydrazine oxidation as the Pd UME does if the potential < 0.1 V and > -0.5 V; and more electrocatalytic activity for the hydrazine oxidation more than the Pd UME does if the potential >0.1 V. Thus, it could theoretically be predicted that the potential range applied is in the range of between 0.1 V and – 0.5 V, the Pd NPs and the Pt UME would present the same electrocatalytic activity. And, if on the other hand if the potential applied is in the range of >0.1 V, the Pd NPs colliding on the Pt UME would present less electrocatalytic activity therefore generating a decline of the absolute value of the current.

As previously mentioned, the single Pd NP collision experiments were performed by using Carbon fiber, Cu, Ni, Pt, and Au UMEs for comparison.

The applied potentials of 0.1 V at all these UMEs were used to minimize the value of the background current. Figure 15 shows the background currents observed both at 0.1 V and 0.3 V. Figure 16 shows Chronoamperometric curves for single Pd NP collisions applied at 0.1 V on the different UMEs. As It can be noticed from figure 15, an application of higher voltages leads to a higher background current.

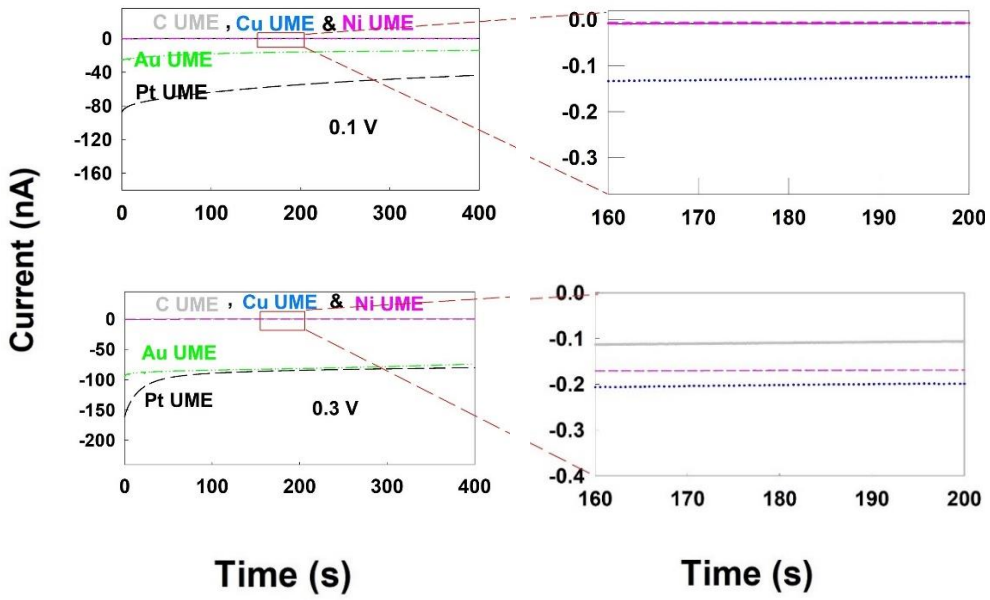

Figure 15. Background currents for the Chronoamperometric measurements in a 50 mM PB solution containing 15 mM hydrazine and at a pH of 6.8. The data acquisition time is 50 mV. s^{-1}

Our experimental results showed that the collision-related signals occurred for all the UMEs. As shown in Figure 16, current response signals of transient features were observed at 0.1 V applied at the C and Ni UMEs. These transients blip responses in a single Pd NP collision were previously reported

on these UMEs. It is highly possible that the metal-nonmetal interaction between the C UME and the PdNPs must be the reason why these transient currents are observed with the C UME collision signals. However, this reason is not very relevant when it comes to the signals observed in the Ni UME.

Given that both the Ni UME and the Pd NPs have both metallic properties, there must be another reason why these transient current patterns are observed. Very low intensity blip current responses from the current signal of a single Pd NP collision were observed when a Cu UME was used as the inert electrode. Au and Pt UMEs on the other hand to show some display some staircase signals. Secondly, the responses with transient features occurred for C and Ni UMEs. Interpreted from another perspective, it can also be stated that Signals on C and Ni UMEs did not show very distinct blip-like or staircase-like features. However, the transient responses obtained at the C UME manifested different characteristics, such as potential dependence, charge transfer amount, and collision frequency, compared to the case of Ni UME. These differences in the transient responses observed in the C and Ni UMEs cases should be explained based on a different mechanism than in the C and Ni UMEs. We will discuss this later.

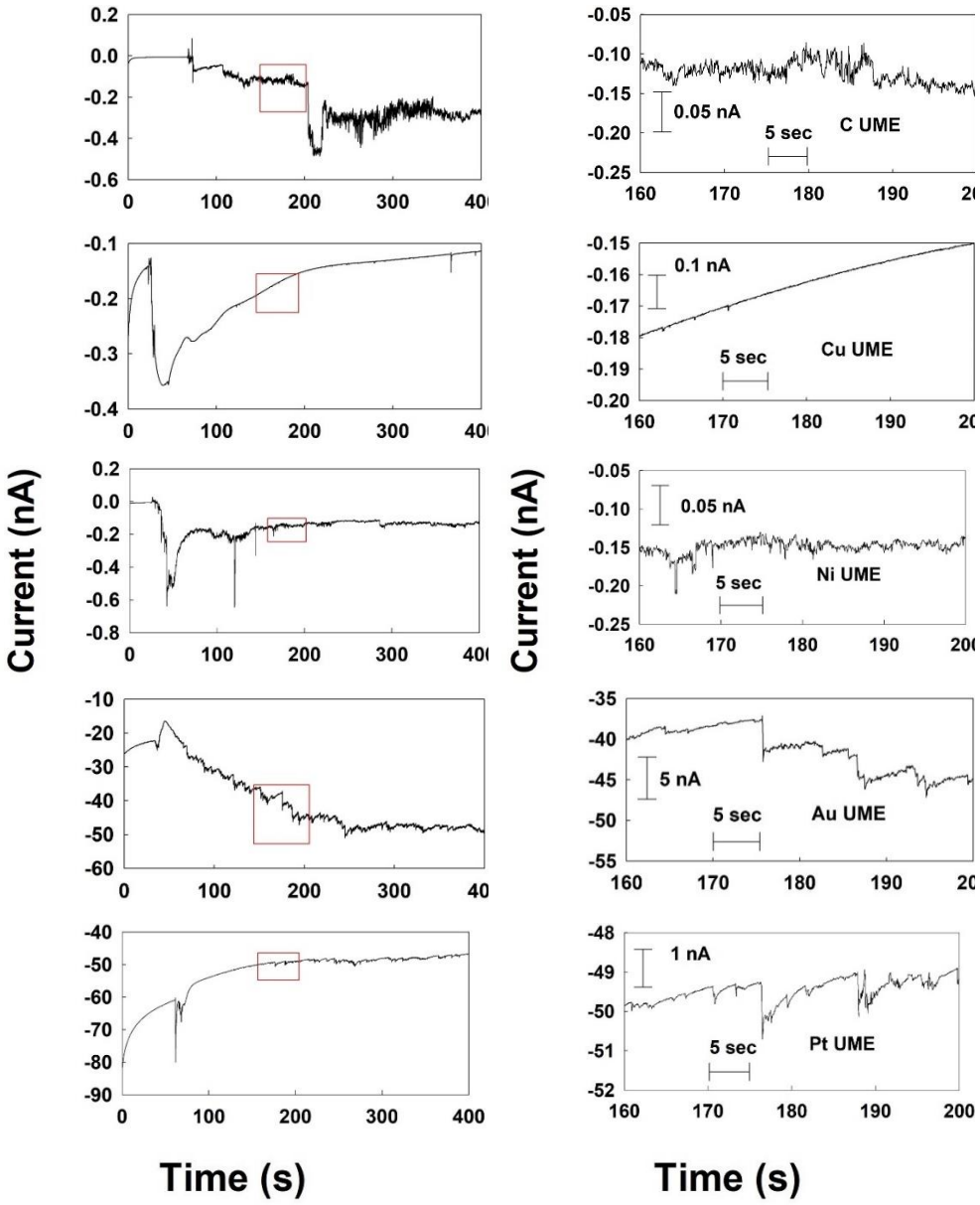

Figure 16. Chronoamperometric curves for single Pd NP collisions applied at 0.1 V on the GC, Cu, Ni, Au and Pt UMEs with the Pd NP concentrations 246 pM in a 50 mM PB solution containing 15 mM hydrazine and at a pH of 6.8. The data acquisition time is 50 mV. s^{-1}

As previously mentioned, current responses at the Au and Pt UMEs were in form of staircases. Particularly, it was at the beginning hard to predict with the Pt UME, there could be the possible generation of these ECA collision signals. That is because as it can be seen from the cyclic voltammograms (Figure 14) of the Pd and Pt UMEs, the CVs of both materials do not seem to overlay over a wide range of voltage (from 0.1 V to -0.5 V) but their CVs also do not display any significant difference of current gap at this operating voltage of 0.1 V.

For the Carbon fiber, Cu, Pt, and Ni UMEs, the potential can be applied over a wide range of potentials (0–0.4 V). Therefore, we tried to find out whether the change in the current response would be if we applied different potentials other than 0.1 V. We carried out our experiments with a potential of 0.3 V. Although in the case of Au, and Pt, there seemed to be some very some blip-like signals observed, the general trend of the experimental results showed that no consistent collision currents are obtained with Carbon fiber, and Cu UMEs. Similar low signal trends had already seemed to have been observed with the Cu UME when 0.1 V was applied. These negative results at 0.3 V for the Carbon fiber and Cu UMEs are however in contrast with the results that had been previously observed with at 0.1 V. As previously pointed out, in the other cases of our investigation at the potential of 0.3 V, blip-like responses were observed with the Au and Pt UMEs. All these results at the potential of 0.3 V can be visualized in figure 17.

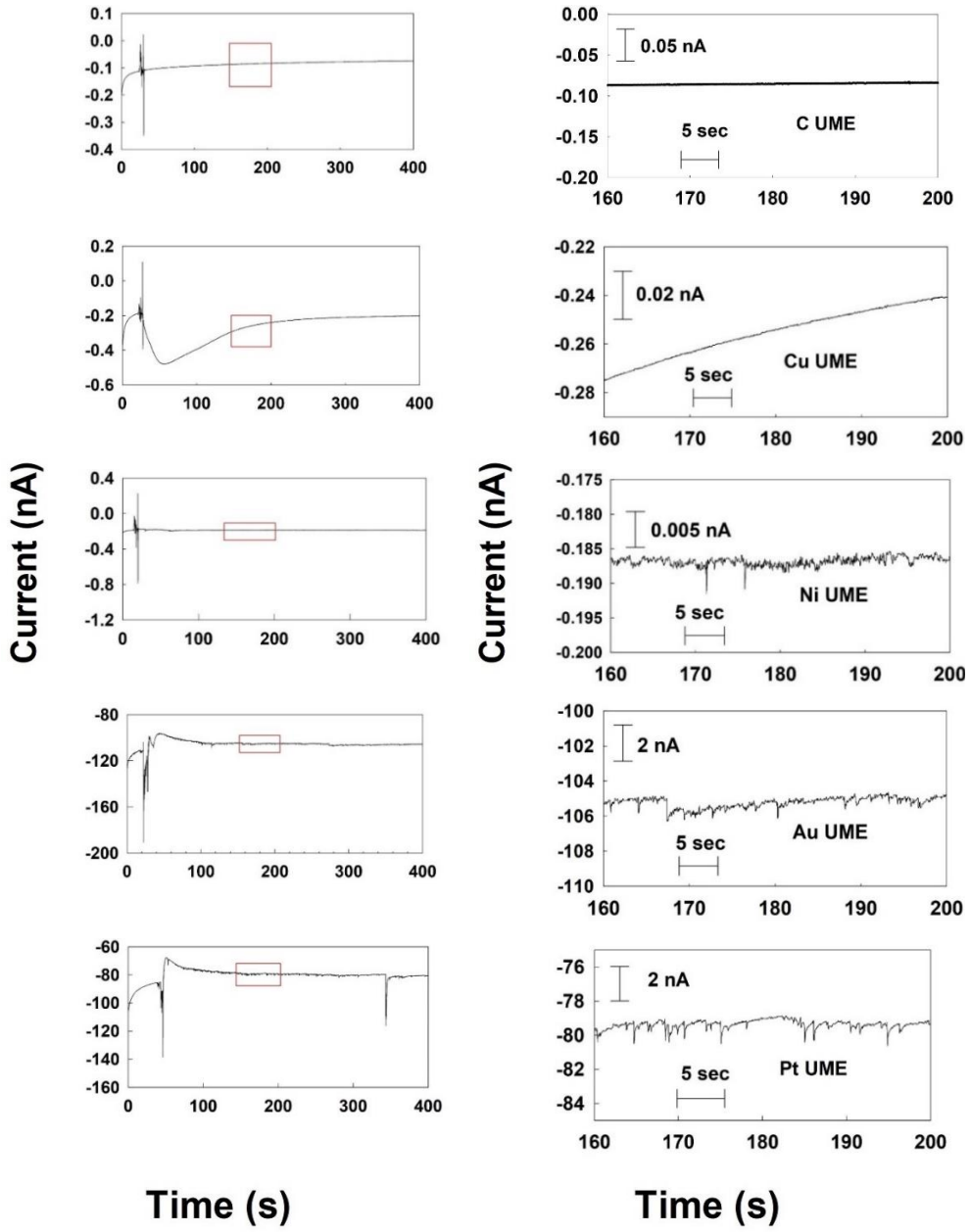

Figure 17. Chronoamperometric curves for single Pd NP collisions applied at 0.3V on the GC, Cu, Ni, Au and Pt UMEs with the Pd NP concentrations 246 pM in a 50 mM PB solution containing 15 mM hydrazine and at a pH of 6.8. The data acquisition time is 50 mV. s^{-1}

At 0.3V, the shape of the current response in the Au UME was not very different from that obtained in the Pt UME case: all were blip signals. However, even though there were no consistent difference in the overall shapes of the UMEs signals; the peak heights observed did not seem to be in the same range. The peak heights observed in the Au UME collision signals seemed to be more pronounced than those observed in the Pt UME collision signals. Also, the current responses of Pd NP collision on UME of the same type at 0.3 V differed from the one obtained at 0.1 V. For the Au UME, the current response is less staircase with some more pronounced blip-like features at 0.3 V, and that is different from the staircase signal obtained when the applied potential is 0.1 V. For the Pt UME, the current response observed at 0.3 V had more blip patterns compared to the one observed at 0.1V which instead presented more staircase like features. These overall differences between the signals obtained at 0.1 V and 0.3 V must be due to fact that the transferred charge per single transient current at 0.1 V is larger than that at 0.3 V.

If one compares the chronoamperogramms at 0.3 V and those at 0.1 V, the observations also come to reveal that application of voltages that are both greater (or equal) and very close to the onset voltage is better suited for the Amperometric detection of the collision events. In our early experiments, we did not use 0.25 V, 0.2 V or 0.15 V. We have instead used 0.1 V as a value that is both close and equal to the onset voltage predicted by analysis of the cyclic voltammograms. As we will explain it in one of the next paragraphs, the recordable minimum size of the transient current depends on the background current level at the UME. If application of higher voltages can produce higher collisions ECA currents, they also induce at the same time higher background currents which can make the electro detection more difficult or impossible to realize. The types of collisions signals obtained both at 0.1 V and 0.3 V are summarized in table 4.

UME	**Response Type at 0.1 V**	**Response Type at 0.3 V**
C	Staircase, blip	no signal detected
Cu	Blip	no signal detected
Ni	Staircase, blip	Staircase, blip
Au	Staircase	Blip
Pt	Staircase	Blip

Table 4. Response types of single Pd NPs collisions at C, Cu, Ni, Au, and Pt UMEs obtained during the chronoamperometric measurements at 0.1 V and 0.3 V.

As previously mentioned, current response signals of transient features were observed at 0.1 V applied at the C and Ni UMEs. And for these UMEs, the frequency count approximation was achieved by focusing on the main transient features observed. When accounting for the noisy-like transient features observed in the C and Ni UMEs, the C UME seems to present the highest frequency count. However, if one neglects these noisy-like transient features, the experimental values of the frequency of single NP collisions were found to be the highest with the Au UME case and the lowest with the Pt UME case. When it comes to Cu and Ni UMEs, they presented collision frequency values in the intermediate range between values of the previous ones. While maintaining the same concentration of Pd NPs, the trend observed within the collision frequencies of the Pd NPs collisions at various UMEs are shown in Table 5. The theoretically expected collision frequency f_p and peak height I_{SS} which are exposed in Table 5, were calculated using the following equations:

$$f_p = 4k_{ads}r_{UME}D_{NP}C_{NP}$$

$$I_{SS} = 4\pi(\ln 2)nFD_{N2H4}C_{N2H4}r_{NP}$$

where k_{ads} is the adsorption coefficient of the Pd NP on the UME, $r_{UME}$is the radius of the UME, $D_{NP}$is the diffusion coefficient of the Pd NP, and C_{NP} is concentration of the Pd NP, n is the number of electrons, D_{N2H4} = is the diffusion coefficient of hydrazine, C_{N2H4} is the concentration of hydrazine, and r_{NP} is the radius of NP.

For the Carbon fiber, Cu, Ni, Au, and Pt UMEs, the theoretically calculated normalized collision frequency at 246 pM for *C*NP was 65.75 s^{-1}. μm^{-1}, when the k_{ads} is considered as 1. If we compare that value with those obtained experimentally, it is found that they differ in hundreds of orders of magnitude with the experimentally obtained values under the same conditions. The presence of various adsorption coefficients can explain the differences between the theoretical values and the experimentally obtained values. As previously stated, the current response features, for example, the response type, collision frequency, and peak height, vary according to the type of UME that was used as an electrode. To better understand the Pd single NP collisions and the effect of electrode material, the results of single Pd NP collision on Carbon fiber, Cu, Ni, Au, and Pt UMEs were compared to the results previous investigations in which different types of UMEs were used.

The collision frequencies and the peak heights of current signals at 0.1 V are listed in Table 5. As it can be noticed, very little collision signals peak heights were obtained with the Cu UME. The spike height of the transient responses at the carbon fiber or Ni UME and the steady-state current magnitude of staircase response at the Cu, Au and Pt UMEs were considered as for the “peak height”, as listed in Table 5. As shown in Table 5, the experimentally obtained average normalized peak height at the C, Cu, Ni, Au, and Pt UMEs

are respectively 0.77, 0.03, 0.11, 21.09, and 13.14 nA.μm. It has been noticed that while the values of peak height obtained when experimenting with the C, Cu, and Ni UMEs are several times smaller than the theoretical calculation, on the other hand, the values obtained with the Au and Pt UME are also greater than the theoretical one and far greater than the experimental values of C, Cu, and Ni UMEs. One possible explanation to this observation is the fact that the lattice properties (atoms sizes and distances) in Au and Pt materials must be very close to those of Pd material, thus facilitating the interaction between their UMEs and NPs.

UME	**Normalized frequency (s^{-1}. μm^{-1})**		**Normalized peak height (nA . μm)**	
	Theoretical estimation	Experimental data	Theoretical estimation	Experimental data
C	65.75	0.030	4.33	0.77
Cu	65.75	0.011	4.33	0.03
Ni	65.75	0.011	4.33	0.11
Au	65.75	0.019	4.33	21.09
Pt	65.75	0.004	4.33	13.14

Table 5. Normalized collision frequencies and peak heights of single Pd NPs collisions at C, Cu, Ni, Au, and Pt UMEs obtained during the chronoamperometric measurements at 0.1V.

The collision frequency of Pd NP on all these UMEs was compared was also compared to the theoretical values. The theoretical frequencies on these UMEs were several orders of magnitude different from the frequencies obtained experimentally as listed in Table 5. Generally, the difference in the collision frequencies is explained as due to the different adsorption coefficients

between Pd NPs and various UMEs. The theoretical collision frequency calculations assumes that Pd NPs collides with the UMEs after an adsorption has occurred. Let us remind that the theoretical calculations in table 5 are approximative and were carried out assuming that Ni, Au, and Pt have the same coefficient of diffusion. These calculations did therefore not consider the different coefficient of diffusion that the nanoparticles may present on the different UMEs. This is the reason why many UMEs with same values of diameter ends up having the same value in table 5. Although we did not push it further and make an estimation of the real adsorption coefficients between Pd NPs and each UME; the collision experimental data can be used to infer about adsorption coefficient of Pd NPs on the various UMEs while operating in a hydrazine solution.

It is important to note that not all the collision-related features are explained by the diffusion of Pd NPs on the UME. Thus, any other factor not considering the surface state of UME (and therefore the adsorption coefficient) should also be included in the estimation of the collision frequency. In previous studies it has been speculated that in the case of Cu UME, the surface is not always in a stable state because the self-oxidation and its reduction back by hydrazine continuously that can take place at some voltages. Thus, the unstable surface state of Cu UME can diminish its adsorption coefficient (Jung et al. 2016). Even though our investigations did not cover the other adsorptive particularities which could be associated to the C, Ni, Au or Pt UMEs, these particularities could also potentially be some other additional non-diffusion related reasons why there is some disparities between their theoretical values of C, Ni, Au or Pt UMEs, and their experimental values.

As recorded, we have observed some particular noise-like patterns in the collision signal of the C and Ni UMEs. We then conducted some extra experiments to find whether those noisy features appear due to an oxidation of the Ni UME contact surface or are otherwise present within the original non-

oxidized Ni UME surface. We proceeded to two different Amperometric measurements, one preceded by an electrochemical reduction of the Ni UME contact surface and the other by an electrochemical oxidation of the Ni UME contact surface. The experimental results showed that the noisy-like features in the collision signals are present whether the contact surface is oxidized or not. These results made us conclude that the transient nature of the collision signals observed when Pd NPs collide with the Ni UME are due to some other factor other than the oxidation or non-oxidation state of the UME surface material. There was no further experimental set up to conducted for the investigation of the transient response observed with the C UME.

In the experimental investigations of collision frequency, one other important factor to estimate was the background current level of the UMEs. The reason is because if the current signal by a single NP collision is relatively very small; it can be hidden in the background current when the latter is elevated. Thus, the recordable minimum size of the transient current has some dependency with the background current level at the UME. And this another major reason why we performed most of the collision experiments at a voltage which could generate the possible lowest background current, that is 0.1 V. For applied voltages of 0.1 V, most measurements presented a relatively small background, and the detection of collisions signals was possible. In every session where the applied voltages were 0.3 V, the background currents in some cases seemed to show values greater than the actual collision run signals, and the detection of the Pd NPs collisions was not possible. We suspect that the high value of the background current obtained in Cu UME experiments must be the same reason why we did not obtain consistent Pd NPs collision signals. Previous studies have even confirmed that for Cu UME, the surface oxidation of Cu UME makes the background current high, and the possibility of loss of the small size of current transient from the small size of NP increases. (Jung et al. 2016). Although we did bring any direct evidence that the same phenomena occurs for the C UME as well, we think that there

is a very probability that the same phenomenon happens as well.

While the background current may play a very important role in explaining the various behaviors observed, it does however not explain why we have sometimes obtained signals at the Au and Pt UMEs when higher voltages (0.3 V) were applied. If our earlier reasoning was right, the higher background current obtained at 0.3 V should make collision signals more difficult to detect in Au and Pt UMEs than it is for the C, Ni and Cu UMEs. We as well can think that there is a very probability that the phenomenon of NP-UME surface interaction is very important as well in determining the outcome of the collision signals observed.

Chapter 5. Conclusion

To sum up with an overall look at our scientific investigation, we did find that single Pd NP collisions were observed at various inert and active electrodes, which in our case were carbon fiber, Cu, Ni, Au, and Pt electrodes. Our first major observation was the fact that the current response type, the collision frequency, and the peak height are highly affected by the material of the UME. From the experimental data, we have been able to predict the mechanism of Pd NPs collision on the UMEs and provide a better comprehension of the nature of many of the single Pd NP collisions. Although we did not merge into more details regarding the adsorption coefficients between Pd NPs and the UMEs; their real and closest values can as well be predicted from the experimental data. We have noticed that application of smaller voltages that are both greater and very close to the onset voltage is better suited for the amperometric detection of the collision events. We have also observed that contrary to the C, Cu, and Ni UMEs which did not always display quality and reproducible signals for the Pd NPs, the best chronoamperometric collision signals of Pd NPs were obtainable with the Au and Pt UMEs.

References

ADAMS, B.D. and CHEN, A., 2011. The role of palladium in a hydrogen economy. *Materials today,* **14**(6), pp. 282-289.

ALLERSTON, L.K. and REES, N.V., 2018. Nanoparticle impacts in innovative electrochemistry. *Current Opinion in Electrochemistry,* **10**, pp. 31-36.

BARD, A.J., BOIKA, A., KWON, S.J., PARK, J.H. and THORGAARD, S.N., 2015. Stochastic events in nanoelectrochemical systems. *Nanoelectrochemistry.* CRC Press Boca Raton, FL, pp. 241-292.

BARD, A.J., ZHOU, H. and KWON, S.J., 2010. Electrochemistry of single nanoparticles via electrocatalytic amplification. *Israel Journal of Chemistry,* **50**(3), pp. 267-276.

CHEN, A. and OSTROM, C., 2015. Palladium-based nanomaterials: synthesis and electrochemical applications. *Chemical reviews,* **115**(21), pp. 11999-12044.

CHOI, Y.S., JUNG, S.Y., JOO, J.W. and KWON, S.J., 2014. Observation of Electrocatalytic Amplification of Iridium Oxide (IrO x) Single Nanoparticle Collision on Copper Ultramicroelectrodes. *Bulletin of the Korean Chemical Society,* **35**(8), pp. 2519-2522.

COOKSON, J., 2012. The preparation of palladium nanoparticles. *Platinum Metals Review,* **56**(2), pp. 83-98.

DARYANAVARD, N. and ZARE, H.R., 2017. Single palladium nanoparticle collisions detection through chronopotentiometric method: introducing a new approach to improve the analytical signals. *Analytical Chemistry,* **89**(17), pp. 8901-8907.

FAULKNER, L.R. and BARD, A.J., 2002. *Electrochemical methods: fundamentals and applications.* John Wiley and Sons.

HASSAN, K., HATHOOT, A., MAHER, R. and AZZEM, M.A., 2018. Electrocatalytic oxidation of ethanol at Pd, Pt, Pd/Pt and Pt/Pd nano particles supported on poly 1, 8-diaminonaphthalene film in alkaline medium. *RSC advances,* **8**(28), pp. 15417-15426.

JIANG, K., ZHANG, H., ZOU, S. and CAI, W., 2014. Electrocatalysis of formic acid on palladium and platinum surfaces: from fundamental mechanisms to

fuel cell applications. *Physical Chemistry Chemical Physics,* **16**(38), pp. 20360-20376.

JUNG, S.Y., JOO, J.W. and KWON, S.J., 2016. Observation of Blip Response in a Single Pt Nanoparticle Collision on a Cu Ultramicroelectrode. *Bulletin of the Korean Chemical Society,* **37**(3), pp. 349-354.

KWON, S.J., FAN, F.F. and BARD, A.J., 2010. Observing iridium oxide (IrO x) single nanoparticle collisions at ultramicroelectrodes. *Journal of the American Chemical Society,* **132**(38), pp. 13165-13167.

MANDLER, D., 2010. *Fritz Scholz (Ed.): Electroanalytical methods.Guide to experiments and applications,* .

MUN, S.K., LEE, S., KIM, D.Y. and KWON, S.J., 2017. Various Current Responses of Single Silver Nanoparticle Collisions on a Gold Ultramicroelectrode Depending on the Collision Conditions. *Chemistry–An Asian Journal,* **12**(18), pp. 2434-2440.

OJA, S.M., WOOD, M. and ZHANG, B., 2013. Nanoscale electrochemistry. *Analytical Chemistry,* **85**(2), pp. 473-486.

PARK, J.Y., KIM, K.J., SON, H. and KWON, S.J., 2018. Chronoamperometric Observation and Analysis of Electrocatalytic Ability of Single Pd Nanoparticle for Hydrogen Peroxide Reduction Reaction. *Nanomaterials,* **8**(11), pp. 879.

STEPHEN, A.J., REES, N.V., MIKHEENKO, I. and MACASKIE, L.E., 2019. Platinum and Palladium Bio-Synthesized Nanoparticles as Sustainable Fuel Cell Catalysts. *Frontiers in Energy Research,* **7**, pp. 66.

STANISLAV V. SOKOLOV, SHALTIEL ELOUL, ENNO KÄTELHÖN, CHRISTOPHER BATCHELOR-MCAULEY and RICHARD G. COMPTON. Issue 1, 2017. Electrode–particle impacts: a user's guide. Physical Chemistry Chemical Physics.

SUNDAR, S., KIM, K.J. and KWON, S.J., 2019. Observation of Single Nanoparticle Collisions with Green Synthesized Pt, Au, and Ag Nanoparticles Using Electrocatalytic Signal Amplification Method. *Nanomaterials,* **9**(12), pp. 1695.

WALSH, D.A., LOVELOCK, K.R. and LICENCE, P., 2010. Ultramicroelectrode voltammetry and scanning electrochemical microscopy in room-temperature ionic liquid electrolytes. *Chemical Society Reviews,* **39**(11), pp. 4185-4194.

WEICHENG, RICHARD G. COMPTON. June 2014. Electrochemical detection of nanoparticles by ‘nano-impact’ methods. TrAC Trends in Analytical Chemistry Volume 58, Pages 79-89

XIAO, X. and BARD, A.J., 2007. Observing single nanoparticle collisions at an ultramicroelectrode by electrocatalytic amplification. *Journal of the American Chemical Society,* **129**(31), pp. 9610-9612.

XIAO, X., FAN, F.F., ZHOU, J. and BARD, A.J., 2008. Current transients in single nanoparticle collision events. *Journal of the American Chemical Society,* **130**(49), pp. 16669-16677.

YAQOOB, S.B., ADNAN, R., KHAN, R.M.R. and RASHID, M., 2020. Gold, silver, and palladium nanoparticles: a chemical tool for biomedical applications. *Frontiers in chemistry,* **8**.

APPENDIX

FORMULAS USED IN THE CALCULATIONS

Most of the calculations involved in our research were obtained from some operations relying on some key scientific formulas. Although some of these formulas are already presented in the previous texts, we thought it might be a good idea to present all these as well as the succession of the operations involved in the calculations. Wherever necessary, the derivation of some key formulas is also presented.

PARAMETER	FORMULA
Diffusion coefficient of the nanoparticles	$$D_i = \frac{kT}{6\pi\eta a}$$ where: *k* is the Boltzmann constant, η is the viscosity of solution, *a* is the radius of a species. In aqueous solution and at normal temperatures, we will have: $$D_i = \frac{1.38064852 \times 10^{-23} \times 298}{6 \times 3.14 \times 8.90 \times 10^{-4} \times a}$$
UME radius	$$r = \frac{I_{ss}}{4 \times n \times F \times D_{FeCM} \times C}$$ where: I_{ss} is the steady state current obtained while running the cyclic voltammogram in ferrocene methanol solution; n : the number of electrons exchanged during the electrochemical reaction; F: the constant of Faraday; D_{FeCM}: the diffusion coefficient of ferrocene methanol; C : the concentration of the ferrocene methanol solution

$$D_{N2H4} = \frac{I_{ss}}{4.n.F.C.r}$$

where

Diffusion coefficient of Hydrazine D_{N2H4}

D_{N2H4}: the diffusion coefficient of hydrazine
I_{ss} is the steady state current obtained while running the cyclic voltammogram in hydrazine solution
n : the number of electrons exchanged during the electrochemical reaction
F: the constant of Faraday
C : the concentration of the hydrazine solution

Nanoparticles Original Concentration

[continued]

The number N of particles of Nanoparticles present in the prepared solution is given by:

$$N = n_0 \times f_d \times N_A \qquad (1)$$

where:

n_0: is the original number of moles of metal composing the nanoparticles
f_d: is the decreasing factor due to the aggregation of the nanoparticles
N_A : is the Avogadro number. That is the number of particles present within one mole of entities

Since we have:

$$n_0 = \frac{m}{M_m} \qquad (2)$$

$$f_d = \frac{m_{at}}{m_{NP}} = m_{at} \times \frac{1}{m_{NP}} = \frac{M_m}{N_A} \times \frac{1}{m_{NP}} = \frac{M_m}{N_A \times m_{NP}} \qquad (3)$$

Substituting expressions (2) and (3) in expression (1) gives:

$$N = \frac{m}{M_m} \times \frac{M_m}{N_A \times m_{NP}} \times N_A \qquad (4)$$

$$N = \frac{m}{m_{NP}} \qquad (5)$$

And the Concentration of Nanoparticles (in the Prepared solution) $C_{NP(prep)}$ expressed as the number of particles present per unit of solution will be given by:

$$C_{NP(prep)} = \frac{N}{V_s} \qquad (6)$$

$$C_{NP(prep)} = N \times \frac{1}{V_s}$$

$$C_{NP(prep)} = \frac{m}{m_{NP}} \times \frac{1}{V_s}$$

Nanoparticles Original Concentration

[continued]

$$C_{NP(prep)} = \frac{m}{m_{NP} \times V_s} \qquad (7)$$

The Concentration of Nanoparticles in the Prepared solution $C_{NP(prep)}$: expressed as the number of moles of particles present per unit of solution will be given by:

$$C_{NP(prep)} = \frac{m}{m_{NP} \times V_s \times N_A} \qquad (8)$$

where: N_A: is the Avogadro number. That is the number of particles present within one mole of entities

$$C_0 = C_{NP(prep)}$$

The Concentration of Nanoparticles in the Prepared solution $C_{NP(prep)}$:
expressed as the number of moles of particles present per unit of solution and assuming all the nanoparticles are spherical will be obtained from expression (8).

$$C_{NP(prep)} = \frac{m}{m_{NP} \times V_s \times N_A}$$

$$C_{NP(prep)} = \frac{m}{\rho_{NP} \times V_{NP} \times V_s \times N_A}$$

$$C_{NP(prep)} = \frac{m \times (N_A)^{-1}}{\rho_{NP} \times 4/3 \times \pi \times (r_{NP})^3 \times V_s}$$

And the final operations give us the formula used to calculate the concentration of the nanoparticles in the prepared solution. We get:

Nanoparticles Original Concentration

[continued]

$$C_{NP(prep)} = \frac{m \times (N_A)^{-1}}{\rho_{NP} \times 4/3 \times \pi \times (r_{NP})^3 \times V_s} \quad (9)$$

$$f = 4 D_s C_s r$$

where

f is the collision frequency in s^{-1}
*D*s is the diffusion coefficient of the particles in cm^2/s
*C*s is the concentration of the particles in cm^{-3}
r is the radius of the electrode in cm

If we are dealing with the nanoparticles palladium, the above formulas becomes:

Concentration of the particles in solution

and

the frequency of the collisions

$$f = 4 \times D_{Pd} \times C_s \times r$$

where

D_{Pd} is the diffusion coefficient of the particles in cm^2/s

C_s is the concentration of the nanoparticles per unit volume of the Cell. (in Moles of Nanoparticle/cm^3)

r is the radius of the electrode (in cm)

If we have a 10 mL cell and Y µL of the nanoparticles are injected, C_s will be given by:

$$C_s = \frac{\text{Number of Moles of Nanoparticles injected}}{\text{Volume of the cell Used}}$$

$$C_s = \frac{\boldsymbol{C_o \times V_{inj}\, \mu L}}{10 \text{ mL}}$$

$$C_s = \frac{\boldsymbol{C_o \times V_{inj}\, \mu L \times 10^{-3} cm^3/\mu L}}{\boldsymbol{10\ mL \times 1\ cm^3/mL}}$$

Concentration of the particles in solution

$$C_s = \frac{\boldsymbol{C_o} \times \boldsymbol{V_{inj}} \times \mathbf{10^{-3}}}{\mathbf{10}}$$

$$C_s = \boldsymbol{C_o} \times \boldsymbol{V_{inj}} \times \mathbf{10^{-4}}$$

and

the frequency of the collisions

where V_{inj} is the volume injected expressed in μL

So, I such a case, the frequency of collisions can also be written as:

$$f = 4 \times D_{Pd} \times C_s \times r$$

$$f = 4 \times D_{Pd} \times \boldsymbol{C_o} \times \boldsymbol{V_{inj}} \times \mathbf{10^{-4}} \times r$$

[continued]

Or simply:

$$f = 4 \times \mathbf{10^{-4}} \times D_{Pd} \times \boldsymbol{C_o} \times \boldsymbol{V_{inj}} \times r$$

where

$C_0 = C_{NP(prep)}$ is the original concentration of the nanoparticles (in Number of nanoparticles/cm^3)

V_{inj} is the volume injected expressed (in μL)

Step Height

$$I = n\pi(ln2)nFD_0C_0r_0$$

where:

n_0 is the number of electrons transferred
F is the Faraday
D_0 is the diffusion coefficient of reactant
C_0 is the concentration of reactant
r_0 is the radius of the NP.

If the reactant is Hydrazine, we have:

$$I = 4 \times \pi \times ln2 \times n \times F \times D_{N2H4} \times C_{N2H4} \times r_{Pd}$$

Abstract (in Korean)

팔라듐 나노입자의 탄소, 구리, 금, 백금 극미세전극에의 단일 나노입자 충돌 신호에 관한 연구

루다켐와 허버트

화학과

건국대학교 대학원

최근에는 Bard 그룹 등이 UME (Ultramicroelectrode) 표면에서 나노입자 (NP) 충돌을 감지하는 전기 화학적 방법을 연구했습니다. (Bard, Zhou et al. 2010, Allerston, Rees 2018) 불활성 전극, NP 및 전기 촉매 반응의 적절한 조합은 전기 촉매 증폭 (ECA) 방법을 통해 단일 NP 충돌의 관찰을 용이하게 합니다.

Pd NP는 다양한 전기 촉매 활성으로 인해 가장 널리 사용되는 전기 촉매 중 하나입니다.

탄소 섬유 (Daryanavard, Zare 2017) Au, (Park, Kim et al. 2018), Ni (Oja, Wood et al. 2013)과 같은 다양한 물질이 단일 Pd NP 검출을 위한 불활성 전극으로 사용되었습니다.

단일 NP 충돌에 의한 전류 신호 응답 유형은 UME의 재료를 포함한 다양한 요인에 영향을 미쳤습니다. 전극 표면에 충돌하여 부딪친 NP의 전류 신호는 계단 반응을 보였다. 대조적으로, 충돌 된 NP가 부반응을 겪을 때 blip (spike) 반응이 얻어진다. 따라서 반응 속도 및 인가한 전위와 같은 다양한 요소들이 단일 NP 충돌의 전류 신호 응답 유형에 영향을 미칠 수

있습니다. UME의 재료는 단일 NP 충돌에서 전류 신호 응답 유형을 결정하는 중요한 요소입니다. 서로 다른 UME에서 다양한 전류 신호 반응을 관찰 한 것은 NP와 UME 사이의 상호 작용 메커니즘 때문입니다. 전류 신호 모양은 NP의 전기 촉매 능력이 유지되거나 감소했음을 나타냅니다. 계단 반응은 전기 촉매 반응이 계속되어야 합니다. 한편, 블립 반응은 NP와 UME 사이의 불순물 흡착 또는 금속 합금과 같은 어떤 이유로 NP의 촉매 활성이 비활성화 된다는 것을 나타냅니다.

따라서 NP와 UME 간의 상호 작용 또는 NP와 반응 생성물 또는 불순물과 같은 화학 물질 간의 상호 작용은 단일 NP 충돌의 전류 신호를 결정하는 데 매우 중요합니다. 전류 신호뿐만 아니라 충돌 빈도수도 전극 재료의 영향을 받습니다. 충돌 주파수는 UME에서 NP의 흡착 계수에 따라 달라지기 때문입니다.

본 연구에서는 탄소 섬유 (C), 구리 (Cu), 니켈 (Ni), 금 (Au), 백금 (Pt)을 단일 Pd NP 충돌의 전기 촉매 활성 연구를 위한 새로운 전극 재료로 도입했습니다. 다양한 전극에 대한 단일 Pd NP 충돌의 전류 신호 반응을 조사했습니다. Pd NP 충돌에 의한 전류 신호는 UME의 재료 및 인가한 전위에 따라 계단에서 블립 신호로 달라졌습니다. 또한 전류 신호의 크기와 빈도수를 분석하여 비교하여 UME의 종류에 따라 크게 달라짐을 알 수 있습니다.

주제어 : 팔라듐 나노입자, 초미세전극, 하이드라진, 단일나노입자 충돌